Electron Spin Resonance and Ultraviolet Spectral Analysis of UV-Irradiated PVA Films Filled with $MnCl_2$ and CrF_3

H. M. Zidan

Physics Department, Faculty of science at Damietta, Mansoura University, P.O. 34517, New Damietta, Egypt

Received 27 January 2002; accepted 9 June 2002

ABSTRACT: PVA films with various filling levels of CrF_3 and $MnCl_2$ were prepared. ESR and UV/VIS optical analysis were used to shed more light on the structural modification that occur due to filling with different levels and/or UV irradiation. The ESR analysis revealed that the spin configuration of CrF_3, $MnCl_2$, and $CoBr_2$-filled PVA are different. The filling level dependence of ESR parameters was discussed. The UV-VIS spectral analysis for pure PVA shows absorption bands at 265 and 280 nm, which were assigned to the presence of carbonyl groups. The addition of CrF_3 led to the appearance of another bands at 418 and 596 nm. The filling level and/or UV irradiation have no effect on the position of absorption bands but the intensity of these bands has been changed. The addition of $MnCl_2$ led to a new band at about 350 nm due to charge transfer transition. The ligand field parameters and optical energy gaps can be calculated and discussed. The results of optical and ESR analysis indicated that the Cr^{3+} or Mn^{2+} are present in its octahedral symmetrical form within the PVA Matrix. SEM micrographs of CrF_3 filled PVA is discussed. © 2003 Wiley Periodicals, Inc. J Appl Polym Sci 88: 104–111, 2003

Key words: UV–vis spectroscopy; structure; irradiation; filler; ESR

INTRODUCTION

Poly(vinylalcohol) PVA has several interesting physical properties, which are very useful in technical applications. PVA, as a semicrystalline material, exhibits certain physical properties resulting from crystal-amorphous interfacial effects.[1,2]

In many technical applications, the observation of changes in polymer structure allows the best polymer composition and preparation conditions to be chosen to achieve the desired properties of the final product. In the study of physical properties of polymer, electron spin resonance (ESR) and optical spectroscopy have been established as important tools for the investigation of polymer–dopant interactions.[3] ESR spectra have been applied to studying the nature of charge carriers responsible for the observed conductivity. Optical spectroscopy (UV/VIS and IR) has been applied to study the band structure and electronic properties of pure and doped polymer films. The information obtained through ESR and optical spectroscopy can then be utilized to unravel the polymer–dopant interactions.

Additions of the dopant to the polymer matrix modify the energy band gap of these materials depending on the type and magnitude of defect concentration of dopant. These modifications give information pertaining to optical, electronic, and electrical conductivity behavior of polymer. The investigations of optical absorption near the band edge and the resulting absorption spectra impart important information relating to various processes occurring in polymers.[4] The study of optical absorption and particularly the absorption edge is a useful method for the investigation of optically induced transitions and for getting information about the band structure and energy gap of both crystalline and amorphous materials.

The generalized use of polymeric materials in radiation environments has recently increased the interest in the interaction between radiation and dielectric materials. The primary process of the interaction of radiation with matter is the production of ions and electronically excited states of molecules, which in turn, may lead to the formation of free radicals.[5] Exposure of polymers to UV irradiations causes changes in structure and morphology,[6] and hence, in chemical and physical properties. Studies on photodegradation of polymers are important not only academically but also industrially. Many kinds of useful polymers for industrial purposes have been developed recently. Fundamental studies on photodegradation are required to obtain photostable polymers and to estimate the lifetime of polymer materials.

The effects of neutron and γ-radiation on some physical properties of PVA-metal halide compounds, have been reported.[7,8] In addition, the effect of UV irradiation on the structure and morphology of PVA doped with $AgNo_3$ has been studied.[9] In our previous study we investigated the effect of both filling level and the nature of metal halide on structural modifications of PVA films.[10] Continuing this goal we are

Correspondence to: H. M. Zidan (Hmzidan@yahoo.com).

Journal of Applied Polymer Science, Vol. 88, 104–111 (2003)

aiming, in the present article, to shedding more light on these structural modifications by using SEM, UV/VIS spectroscopy and ESR spectra.

EXPERIMENTAL

Sample preparation

The PVA and metal halides used in this work were supplied by Aldrich Chemical Co., Milwaukee, WI. PVA was in the form of powder, has an average molecular weight M_w of 125,000. The present PVA films, with different amounts of chromium fluoride and manganese chloride, were prepared by casting method as follows. PVA powder was dissolved in distilled water (5 wt %) by heating up to 70°C for 3 days. Chromium fluoride or manganese chloride was dissolved also in distilled water and added to the polymeric solution. The solutions were left to reach a suitable viscosity, after which they were casted in glass dishes and left to dry in a dry atmosphere at room temperature. Samples were transferred to an electric air oven held at 60°C for 48 h to minimize the residual solvent. The thickness of the obtained films was in the range (0.1 to 0.2 mm). PVA films filled with CrF_3 mass fractions 0, 1, 3, 5, 10, and 15%, and PVA films filled with $MnCl_2$ mass fractions 0, 10, 15, 20, and 25% were prepared. The filler concentration W (wt %) was calculated from the equation,

$$W(\text{wt }\%) = \frac{w_f}{w_p + w_f} \times 100 \quad (1)$$

where w_f and w_p represent the weight of filler and polymer, respectively.

Physical measurements

Ultraviolet-Visible (UV/VIS) absorption spectra of unirradiated and irradiated samples were carried out in the wavelength range from 200–900 nm using a (Perkin-Elmer UV-VIS) spectrophotometer. The electron spin resonance (ESR) spectra were recorded on a JEOL spectrophotometer (Type JES- FE2XG) at a frequency of 9.45 GHz, using DPPH as a calibrant. Scanning electron micrograph of the studied samples were performed using SEM (JEOL-JSM 6100).The SEM specimens were prepared by evaporating gold onto the film surface after drying under vacuum. Irradiation of the samples was carried out using a monochromatic light source of wavelength 254 nm from a low-pressure mercury lamp Cole- Parmer (100 watts).The distance between the light source and sample was 5.0 cm. The thermal effects of the UV lamp were compensated by regulating the sample temperature to be fixed around 298 ± 1 K.

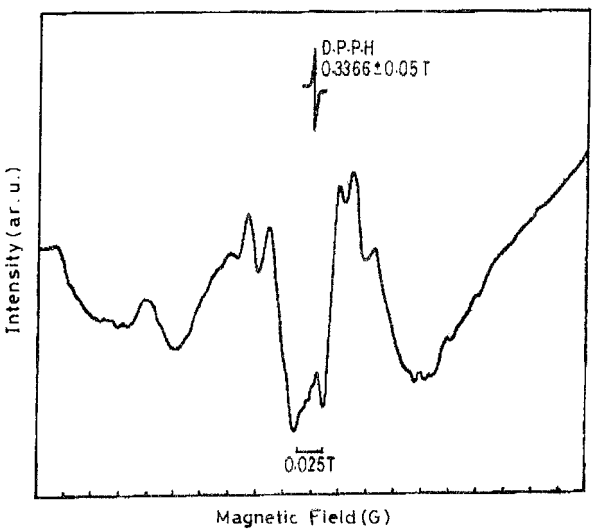

Figure 1 The ESR spectra for pure PVA.

RESULTS AND DISCUSSION

Electron spin resonance (ESR)

The ESR spectrum of unfilled PVA is presented in Figure 1. It is characterized by three main broad signals[11] (due to the pure PVA matrix) with superimposed hyperfine lines (due to free radicals). The obtained spectra may arise from residual free carriers and/or neutral defects in the PVA chain structure. In some of such structural defects[12] the unpaired electron result from a domain wall in the bond alternation resulting in a neutral π-electron free radical. This unpaired electron would be delocalized over several carbon atoms in closer analogy to a domain wall. Such defects could arise principally in the isomerization process of converting *cis*-to-*trans* forms. On the other hand, the ESR may arise from σ-electron radicals, exhibiting a g-factor $< g_e$ (the free electron g-factor).[13] These electrons are expected to be localized in an sp^2 or sp^3 orbital, so the hyperfine splitting from adjacent ^1H or ^{13}C nuclei would be easily distinguished if *trans*-defects occurred in the π-system.

The average rotational correlation time (τ_r) of mobile spins of pure PVA was calculated using the following equation:[11]

$$\tau_r = 6.6 \times 10^{-10}\, w_0 \left[(h_0/h_{-1})^{1/2} + (h_0/h_{+1})^{1/2} - 2\right] \quad (2)$$

where w_0 is the line width of the midfield signal (in Gauss) and h_{-1},h_0 and h_{+1} are the peak-to-peak heights of the low-, central, and high-field signals, respectively. The calculated value of (τ_r) of the present virgin PVA film is 295 ns.

Figure 2 displays ESR spectra of PVA filled with various mass fractions of CrF_3. It is clear that the PVA characterizing spectrum disappeared. The spectra are characterized by a broad Lorentzian signal. The analysis of the present ESR spectra may provide informa-

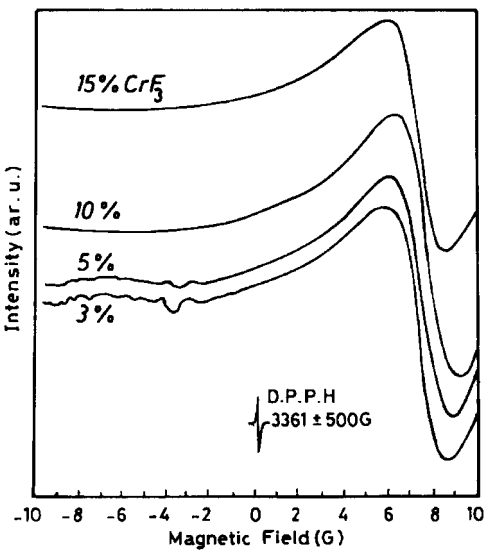

Figure 2 The ESR spectra of PVA filled with various mass fractions of CrF_3.

tion on the distribution of chromium ions in the PVA matrix. The present signals are located around Lande factor (g) $\approx$ 1.82, which is close to the value of g = 2.0037,[14] corresponding to the symmetrical octahedral coordinated Cr^{3+} ions in PVA matrix, coupled by strong dipolar and superexchange interactions.[15]The broad Lorentzian signal is due to the Cr^{3+}–Cr^{3+} exchange interaction, which is caused by the proximity of chromium ions, suggesting[16] the presence of aggregated Cr^{3+}. The filling level dependence of the filler local structure can be clarified more explicitly with the aid of the peak-to-peak separation (ΔH) of the main ESR Lorentzian signal. The obtained values of (ΔH) are plotted as a function of filling level (W) in Figure 3. From this figure we can see that ΔH decreases with increasing (W), which means a sharp ESR signal indicating most ordered Cr^{3+} distribution within the PVA matrix. Using the present ESR spectra, the following parameters were calculated and listed in Table I: the g-factor, the asymmetry factor (F), which is the ratio between the heights of the two halves of the signal, and the spin relaxation time τ (in ms). The deviation of the g-value from 2.00 is partly ascribed to[17] the contribution of orbital angular momentum to the magnetic moment of Cr^{3+}. Table I demonstrates that the filling level dependence of g, F, and τ parameters are nonmonotonic. This may be ascribed to the influence of structural defects, which depend on the mode of filling at various filling levels.[18]

It is worthwhile to compare between the ESR spectrum of the following metal halide-filled PVA:

1. The present system (CrF_3-filled PVA) in which the spectrum characterizing PVA disappeared and was replaced by a single broad Lorentzian signal indicating an aggregated Cr^{3+} forms.
2. The ESR of $MnCl_2$-filled PVA, which were studied previously[17] showed that the spectrum characterizing PVA disappeared. This spectrum was replaced by six lines superimposed on a Lorentzian signal, indicating an isolated Mn^{2+} with an unpaired electron and a significant hyperfine structure of the manganese nucleus (S = 5/2). This was for filling level W $<$ 15%. For filling level W = 15%, a single Lorentzian signal appears, indicating Mn^{2+}–Mn^{2+} exchange interaction within the aggregated Mn^{2+} forms. It is believed that the spectra are well described by S = 5/2 (the free ion spin) and the (trapped) excited electrons of Mn^{2+} (as a multivalent ion) probably interact with OH groups of PVA. This argument is based upon filling level dependence of the OH bending mode noticed in IR analysis.[17]
3. The ESR of $CoBr_2$-filled PVA, which were studied by Tawansi et al.,[3] showed that the spectrum characterizing PVA is not destroyed. The noticed superimposed hyperfine lines are due to the free radicals, whereas the deformation of the main three signals may be attributed to the effect of the filler. The ESR spectra confirm the argument that the electrons are transmitted from the free radical traps to the alcoholic group of PVA. A relatively low percentage of one dimension Ising antiferromagnetic $CoBr_2 \cdot 2H_2O$ microcrystallites, containing spin clusters, which is assumed to be randomly distributed within the PVA matrix. These microcrystallites may induce Ising- like magnetic interactions along the PVA chains.

From the previous discussion, it is clear that the spin configuration of the three systems (CrF_3, $CoBr_2$, and $MnCl_2$-filled PVA) are different. The various behaviors may be attributed to one (or more) of the following factors: (1) the different characters of halides (F, Cl, and Br); (2) the intrinsic features of Cr, Mn, and Co;

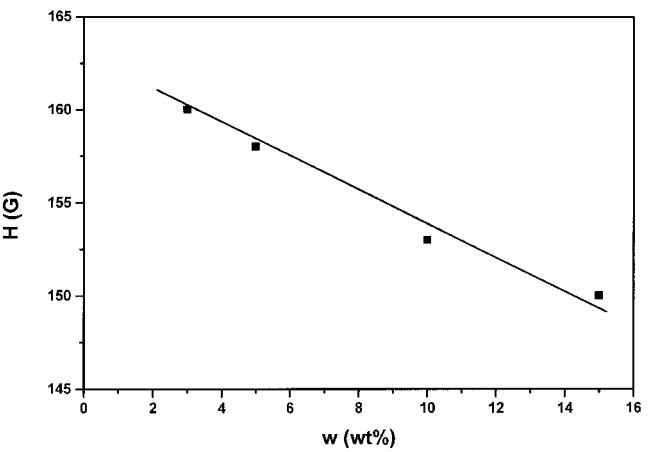

Figure 3 The dependence of the peak-to-peak separation (ΔH) for ESR spectra on filling level (W) of CrF_3.

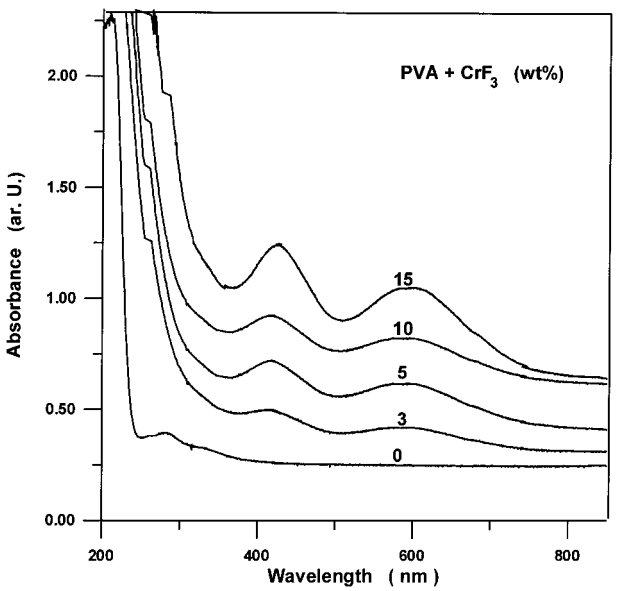

Figure 4 The UV/VIS absorption spectra for films of CrF_3 filled PVA system before UV-irradiation.

and (3) the crystalline and magnetic structures of each halide and their mode of chelation to the PVA chain.

Optical spectroscopy

The UV/VIS spectrophotometric scan in the wavelength range 200–900 nm of pure PVA polymer and filled PVA with various mass fractions of CrF_3, before UV irradiation was recorded and shown in Figure 4. The observed spectra exhibit transitions characterizing PVA, which can be assigned as follow.[9] The spectrum of the unfilled sample contains an absorption peak at 280 nm and a shoulder at about 265 nm. These bands are attributed to carbonyl-containing segments of the general form —(CH═CH)$_n$ CO—, where n = 1,2, . . . , resulting from the presence of acetaldehyde and dissolved air in the vinyl acetate monomer during polymerization. The shoulder at 265 nm is due to the absorption by simple carbonyl groups along the polymer chain. The peak at 280 nm is assigned to the carbonyl groups associated with ethylene unsaturation of the type —(CH═CH)$_2$ CO—, and is indicative of the presence of conjugated double bonds of polyenes.

TABLE I
Filling Level Dependence of the ESR Parameters (g, τ, and F), Calculated Using the Spectra in Figure 2

W (wt)	G	T (ms)	F
0	—	0.295	—
3	1.8179	7.22	0.58
5	1.8211	7.69	0.76
10	1.8126	7.69	0.61
15	1.8204	7.41	0.69

TABLE II
Filling Level Dependence of Wavelength and Intensity of Absorption Bands Observed in Figure 4

W (wt %)	λ (nm)	A	λ (nm)	A	λ (nm)	A
0	265	0.38	—	—	—	—
3	265	1.28	418	0.5	596	0.42
5	265	1.6	420	0.71	598	0.62
10	265	2.3	420	0.91	597	0.8
15	265	2.6	428	1.25	605	1.05

The weaking (or the shoulder form) of this band is due to the presence of isolated carbonyl groups.

For the filled samples, the spectra contain two absorption peaks at about 418 and 596 nm in addition to a shoulder at 265 nm.The disappearance of the absorption band at 280 nm indicates that the concentration of the —(CH═CH)$_2$ CO— carbonyl groups is decreased in the ligand. It is reasonable to assign the absorption bands observed at 596 and 418 nm to the transitions $^4A_{2g} \rightarrow {}^4T_{1g}$, ν_2, and $^4A_{2g} \rightarrow {}^4T_{1g}$ (P), ν_3 respectively.[19] There is no observable change in the band position with filling levels W = 3, 5, and 10 wt % of CrF_3 but for W = 15% of CrF_3, the position of the peaks is slightly shifted towards higher wavelength (Table II). This suggests that the geometry is not altered. On the other hand, the intensity (A) of the absorption peaks increases with increasing filling level, W, as shown in Figure 5. The dependence of the intensity of the bands on the filling level provides an evidence for the incorporation of Cr^{3+} into PVA matrix. From the nature and position of the observed bands, it can be assumed that the Cr^{3+} ion in its octahedral symmetry is responsible for the observed spectrum. This confirms the findings of ESR.

From Figure 4 it is clear that, the pure PVA shows a sharp absorption edge nearly like the crystalline materials at wavelength about 235 nm, while the filled samples with CrF_3 leads to the appearance of an ad-

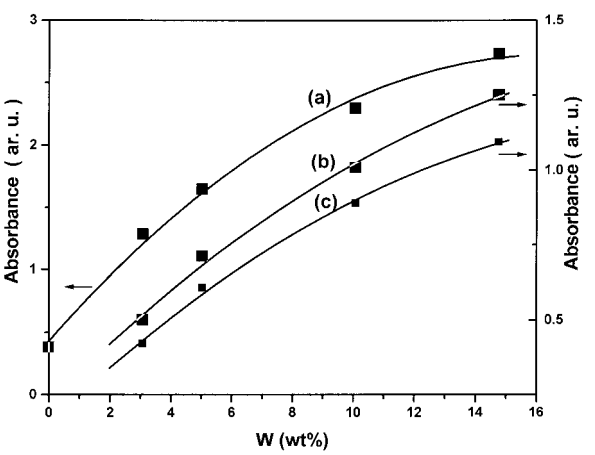

Figure 5 The dependence of absorption intensity peak (A) on filling level (W) of CrF_3, at (a) λ = 265 nm, (b) λ = 418 nm, and (c) λ = 596 nm.

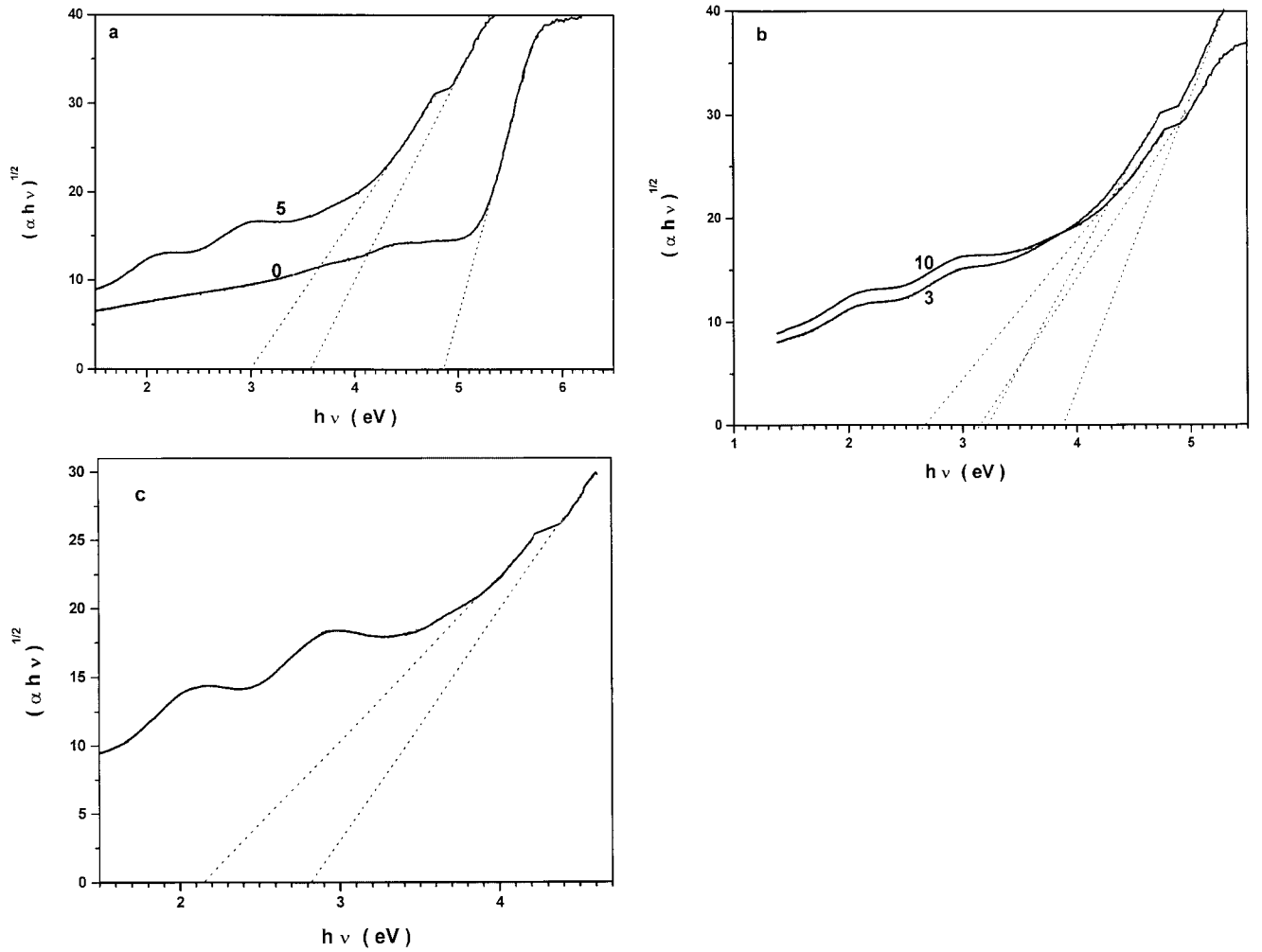

Figure 6 The dependence of $(\alpha h\nu)^{1/2}$ on the photon energy $(h\nu)$ for pure and CrF_3-filled PVA films with different contents.

ditional absorption edge at higher wavelengths. The position of the main edge for the filled samples lies at higher wavelength than that for pure PVA. The absorption coefficient $\alpha(\nu)$, at various frequency values (ν) was calculated using the following formula:[20]

$$\alpha(\nu) = [\ln\{(T_1(\nu)/T_2(\nu)\}/(d_2 - d_1)], \qquad (3)$$

where T_1 and T_2 are the transmittances of two films of the same CrF_3 content with thicknesses d_1 and d_2, respectively. To determine the optical energy gaps for

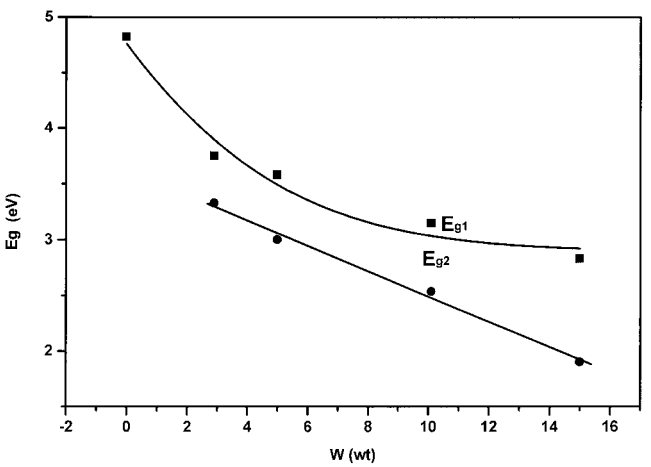

Figure 7 The dependence of the optical energy gaps E_{g1} and E_{g2} on filling level (W) of CrF_3.

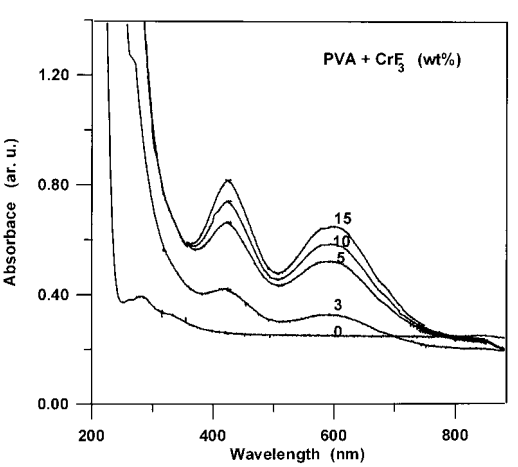

Figure 8 The UV/VIS absorption spectra for films of CrF_3-filled PVA system after UV-irradiation.

TABLE III
Filling Level Dependence of Wavelength and Intensity of Absorption Bands. Observed in Figure 8

W wt %	λ (nm)	A	λ (nm)	A
0	—	—	—	—
3	418	0.42	595	0.32
5	420	0.68	597	0.51
10	420	0.74	597	0.58
15	425	0.81	605	0.65

the studied films, the quantity $(\alpha h\nu)^{1/2}$ is plotted against the photon energy $(h\nu)$ according to Davis and Mott formula:[21]

$$\alpha(\nu) = B'\ (h\nu - E_g)^2/h\nu, \tag{4}$$

where B' is a constant, h is Planck's constant and E_g is the optical energy gap. Figure 6 represents the plot of $(\alpha h\nu)^{1/2}$ vs. $(h\nu)$ for the PVA films containing different contents of CrF_3. This figure shows a linear dependence of $(\alpha h\nu)^{1/2}$ on the photon energy $(h\nu)$ in two regions representing the two optical absorption edges. These absorption edges are characterized by high optical energy gap, E_{g1} and lower energy gap E_{g2}. The values of the optical energy gap, for the studied samples are obtained from the extrapolation of the linear region of the plots to the point $(\alpha h\nu)^{1/2} = 0$. Figure 7 depicts the dependence of E_{g1} and E_{g2} on the CrF_3 content. It is clear that E_{g1} and E_{g2} decrease as the CrF_3 content increases. The variation of the calculated values of both higher and lower optical energy gaps may reflect the role of CrF_3 in modifying the electronic structure of the PVA matrix. In the present study, the observation of two optical absorption edges in the plot of $(\alpha h\nu)^{1/2}$ vs. $(h\nu)$, may be attributed to various polaronic and defect levels. The higher absorption edge, E_{g1} seems to be related to the PVA matrix (ligand), and it changes due to the induced energy states from the octahedral symmetrical field of chromium. These states are characterized by the transitions $^4A_{2g} \rightarrow {}^4T_{1g}$, ν_2, and $^4A_{2g} \rightarrow {}^4T_{1g}$ (P), ν_3, It is argued that the lower absorption edge E_{g2} evidences the presence of another type of induced states depending on the filling level of CrF_3.

The absorption spectra of UV-irradiated pure and filled PVA with various mass fractions of CrF_3 are shown in Figure 8. One can show that the exposure of pure PVA to UV irradiation has no influence on their UV spectral features. Bravar et al.[22] mentioned that even prolonged exposure of PVA to UV irradiation does not provoke neither an increase of the existing bands nor the appearance of new bands. This means practically that under mild conditions of irradiation, the oxidation of PVA is not possible. Rabie and Daghestani[23] concluded that exposure of PVA to γ-irradiation in the range from 0.5 to 5.0 Mrad does not result in the appearance of new infrared absorption bands, but the exposure to 10 and 15 Mrad causes a remarkable increase in the intensity of the carbonyl band at 1710 cm^{-1}. On the other hand, for the filled PVA samples with different mass fractions of CrF_3, no observable shift in the position of the bands has occurred by UV irradiation. However, the absorption intensity of the bands shows a remarkable decrease due to irradiation (see Table III).

The ligand field parameters D_q (splitting energy), B (Racah interelectronic parameter), and β (the ratio B/B_0, where B_0 is the Racah parameter for free ion) for CrF_3 filled PVA films with different mass fractions have been calculated by Tanabe-Sugano procedures[19] and are listed in Table IV using the following equations:

$$B = \frac{1}{510}[7(\nu_3 - 2\nu_2) \pm 3(81\nu_3^2 - 16\nu_2(\nu_2 - \nu_3))]^{1/2} \tag{5}$$

$$D_q = \frac{1}{10}\left[\frac{1}{3}(2\nu_2 - \nu_3) + 5B\right] \tag{6}$$

$$\beta = B/B_0 \tag{7}$$

From the observed electronic transitions, the B values decrease with increasing the filling level and its value is less than that of the free ion (B_0 for $Cr^{3+} = 918$ cm^{-1}). This may be taken as an indication for the formation of metal–polymer complex and to indicate that the ionic bonds formed by Cr^{3+} carry some covalent character and that the effective charge experienced by the d-electrons has been decreased.[19] This may also indicate the increasing degree of overlapping between wave functions of chromium ions and that of the ligand OH group. The decrement of β from unity indicates more covalence for the formed compounds. The values of $(10\ D_q)$, the difference between the t_{2g}

TABLE IV
Filling Level Dependence of Spectral Parameters (B, β, and D_q), Calculated Using the Spectra in Figures 4 and 8

	Before irradiation					After irradiation				
W (wt %)	ν_2 cm^{-1}	ν_3 cm^{-1}	B cm^{-1}	β	D_q cm^{-1}	ν_2 cm^{-1}	ν_3 cm^{-1}	B cm^{-1}	β	D_q cm^{-1}
3	16,779	23,923	746.3	0.813	694	16,807	23,923	746	0.81	696
5	16,722	23,810	742.6	0.809	692	16,750	23,810	743	0.81	694
10	16,750	23,810	742.6	0.809	694	16,750	23,810	743	0.81	688
15	16,529	23,365	728.6	0.794	687	16,529	23,529	734	0.80	685

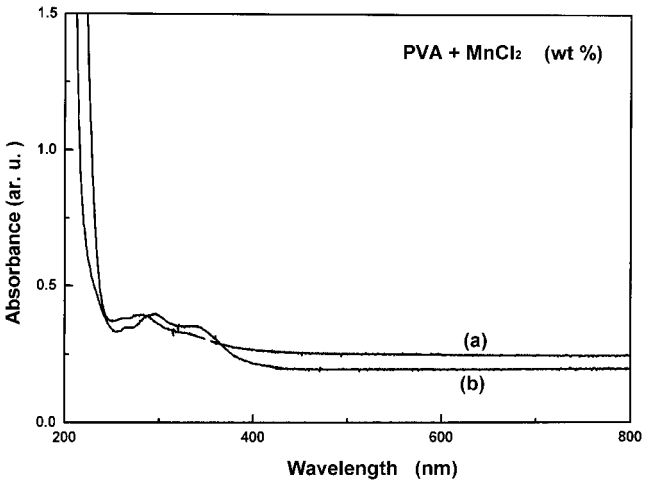

Figure 9 The UV/VIS absorption spectra for films of $MnCl_2$-filled PVA system before UV-irradiation (a) W = 0, (b) W = 5 wt %.

and e_g states in an octahedral structure, were decrease but not pronounced.

The results obtained after irradiation indicate that the values of B, β, and D_q remain unaffected, suggesting that the geometry of the formed compound is not affected by UV irradiation.

The UV/VIS absorption spectra of W = 0 and 5 wt % $MnCl_2$-filled PVA films are shown in Figure 9. Comparing the spectra of pure PVA with that of PVA filled with $MnCl_2$, one can notice that a new band is observed at $\lambda \approx 350$ nm in addition to the band at $\lambda = 285$ nm (which characterizes the virgin polymer). The band at $\lambda \approx 350$ nm is probably due to charge-transfer transition, which may be due to the formation of a new compound [PVA-Mn(11)]. The intensity of this band increases slightly with increasing the filling level. The absence of any band in the visible region is characteristic of the presence of Mn^{2+} in a high-spin octahedral configuration ($t^3_{2g}\ e^2_g$) with spin-forbidden transitions, which is a direct consequence of the presence of spin-orbit coupling. The assigned band positions for the other filling levels (10, 15, 20, and 25 wt % $MnCl_2$)were found to be similar and therefore are not presented here. Also, it is observed that the exposure of filled PVA samples with different mass fractions of $MnCl_2$ to UV irradiation has no influence on their UV spectral features.

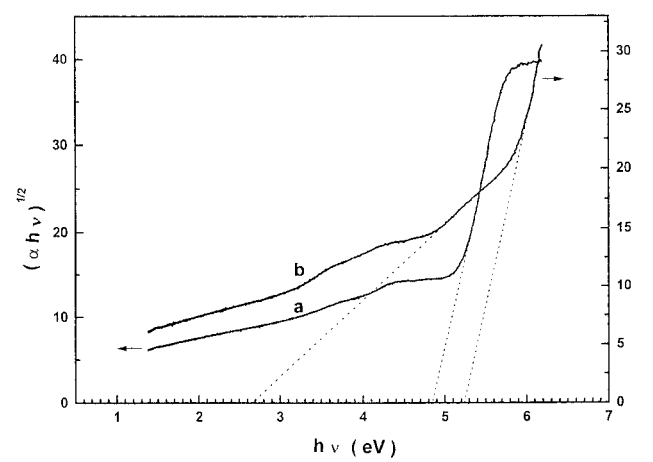

Figure 10 The dependence of $(\alpha h\nu)^{1/2}$ on the photon energy ($h\nu$) for films of $MnCl_2$-filled PVA system (a) W = 0, (b) W = 5 wt %.

TABLE V
Dependence of the Optical Energy Gaps (E_{g1} and E_{g2}) on $MnCl_2$ Filling Level W (wt %)

W (wt %)	0	3	5	10	15
E_{g1}(eV)	4.82	4.63	5.16	5.29	5.18
E_{g2}(eV)	—	3.05	2.61	3.05	3.42

From eq. (3) one can calculate the absorption coefficient α (ν) for $MnCl_2$-filled PVA films with different contents, and consequently the quantity $(\alpha h\nu)^{1/2}$ can be determined. Figure 10 represents the plot of $(\alpha h\nu)^{1/2}$ vs. ($h\nu$) for pure PVA and PVA films containing 5 wt % of $MnCl_2$.This figure shows a linear dependence on photon energy ($h\nu$) in two regions representing two optical energy gaps. The higher energy gap (E_{g1}) is due to the pure PVA and the lower one (E_{g2}) is due to addition of $MnCl_2$. The values of optical energy gaps (E_{g1} and E_{g2}) for pure and PVA filled with different filling levels of $MnCl_2$ are calculated and listed in Table V. It is obvious that the change of the values of the optical energy gaps with increasing $MnCl_2$ content is nonmonotonic. Assuming that energy gaps to be influenced by the induced states due to $MnCl_2$ filling of PVA, one may attribute the optical behavior to the change of the filling mode of $MnCl_2$ chliation to the PVA matrix.

SEM micrography

The SEM micrograph of the morphology of PVA films for various filling levels of CrF_3 is shown in Figures 11 and 12. The micrograph in Figure 11 of unfilled PVA is characterized by normal crystalline with uniformly circular shape (of smooth boundaries and the grown ones are nearly of equal sizes of average diameters ≈ 8

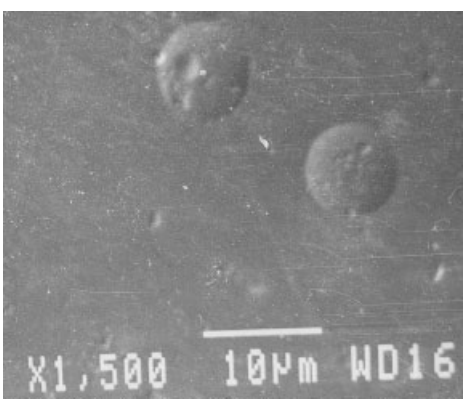

Figure 11 SEM micrograph for pure PVA film.

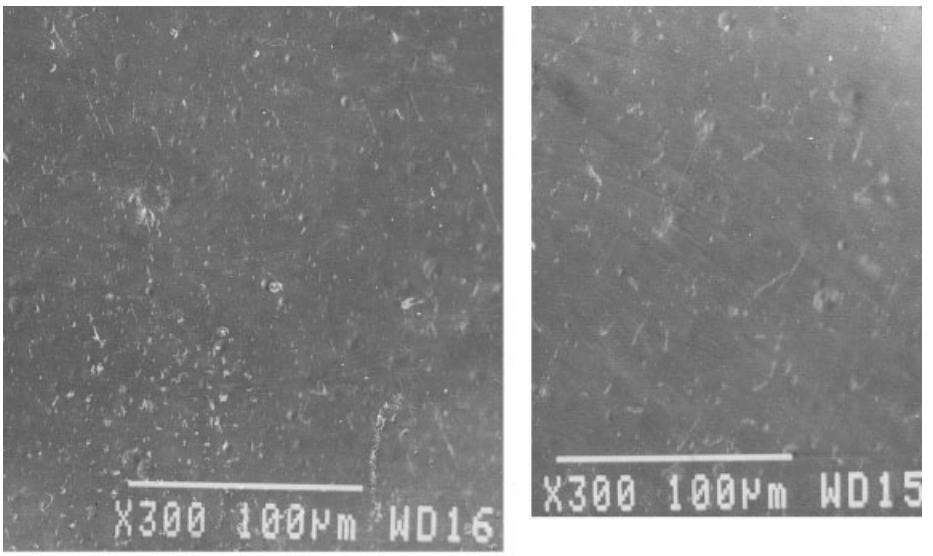

Figure 12 SEM micrograph for PVA films filled with CrF_3 (a) WD16 and (b) WD15.

μm), randomly distributed in a continuous amorphous matrix, and indicating the occurrence of a homogeneous growth mechanism. Figure 12 shows a very thin plate (lamellae) structure, which is distributed in amorphous matrix, beside the original crystalline phase. For filling level W = 5 wt % CrF_3 [Fig. 12(a)], a lamellar structure started to grow homogeneously in the structure with plate average thickness of 1 μm and average spacing of 10 μm, while in the case of W = 10 wt % CrF_3 the thickness and separation of lamellar structure increased to 3 and 13 μm, respectively. The appearance of lamellar structure besides the original crystalline phase indicates the existence of another crystalline phase due to filling of CrF_3.

CONCLUSION

The results of this work showed that there are changes in the measured parameters for the studied samples due to filling or UV irradiation. These changes had been interpreted in terms of the structural modification of the PVA matrix, which depends on the filler content, and the chemical nature of the filler. The ESR results revealed that the spectrum characterizing PVA is not destroyed due to addition $CoBr_2$, contrary to $MnCl_2$ and CrF_3. The distribution of Cr^{3+} is in aggregated form within the PVA matrix, while that of Mn^{2+} is in isolated and/or aggregated modes. Also, it was found that the g-factor < 2.00 indicates the contribution of the orbital angular momentum to the magnetic moment of Cr^{3+}. The UV/VIS spectra revealed two optical energy gaps of filling level dependent width. The higher optical gap characterizes the ligand matrix in either its pure or modified form. The lower optical gap is thought to arise from different induced energy states. The calculated ligand field parameters indicate the formation of metal polymer–complex and the geometry of the formed compound is not affected by UV irradiation. SEM micrographs revealed the appearance of another crystalline phase beside the original PVA crystalline phase.

References

1. Su, I.; Ma, Z. Y.; Scheinbeim, J. I.; Newman, B. A. J Polym Sci Polym Phys 1995, 33, 85.
2. Tawansi, A.; Zidan, H. M. J Phys D Appl Phys 1990, 23, 1320.
3. Tawansi, A.; Zidan, H. M.; Oraby, A. H.; Dorgham, M. E. J Phys D Appl Phys 1998, 31, 3428.
4. Misra, S. C. K.; Beladakere, N. N.; Pandey, S. S.; Ram, M. K.; Sharma, T. P.; Malhotra, B. D.; Chandra, S. J Appl Polym Sci 1993, 50, 411.
5. Krok, J. Radiation Chemistry; Polish Publishing House: Warso, 1975 (in Polish).
6. Kaczmarek, H. Polymer 1996, 37, 189, 547.
7. Abd El-Kader, F. H.; Hamza, S. S.; Attia, G. J Mater Sci 1993, 28, 6719.
8. Abd El-Kader, F. H.; Attia, G.; Ibrahim, S. S. J Appl Polym Sci 1993, 50, 1281.
9. Zidan, H. M. Polym Test 1999, 18, 449.
10. Zidan, H. M.. J Appl Polym Sci, Submitted.
11. Kivelson, D. J Chem Phys 1960, 33, 1094.
12. Goldberg, I. B.; Crow, H. R.; Newman, B. R.; Heeger, A. J.; Diarmid, M. J Chem Phys 1979, 70, 1132.
13. Stone, A. J. Mol Phys 1963, 6, 509.
14. Tanaka, K.; Kamiya, K.; Yoko, T.; Tanabe, S.; Hirao, K.; Soga, N. J NonCryst Solids 1989, 109, 289.
15. Burzo, E.; Chipara, M.; Dngur, D.; Ardelean, I. Phys Stat Sol (b) 1984, 124, K 117.
16. Yano, S.; Yamashita, H.; Matsushita, M.; Aoki, K.; Yamauchi, J. Colloid Polym Sci 1981, 259, 514.
17. Tawansi, A.; Oraby, A. H.; Zidan, H. M.; Dorgham, M. E. Physica B 1998, 254, 126.
18. Yamauchi, I.; Yano, S. Macromolecules 1982, 15, 210.
19. Lever, A. P. B. Inorganic Electronics Spectroscopy; Elsevier: Amsterdam, 1968.
20. Chiodlli, G.; Magistris, A. J Solid State Ionics 1986, 18–19, 356.
21. Davis, E. A.; Mott, N. F. Philos Mag 1970, 22, 903.
22. Bravar, M.; Rek, V.; Kostela-Biffi, R. J Polym Sci Symp 1973, 40, 19.
23. Rabie, S. M.; Daghestani, A. Y. Isotope Radiat Res 1985, 17, 9.